Supporting Information

Sponge-like hierarchical porous carbon decorated by Fe atoms for high-efficient sodium storage and diffusion

Wen-Huan Huang,[a] Zhuo Chen,[a] Hao-Yang Wang,[a] Lei Wang,[a] Hua-Bin Zhang,[b] and Hong Wang,[c]*

[a.] *Key Laboratory of Chemical Additives for China National Light Industry, College of Chemistry and Chemical Engineering, Shaanxi University of Science and Technology, 710021, Xi'an, China. E-mail: huangwenhuan@sust.edu.cn*

[b.] *KAUST Catalysis Center, King Abdullah University of Science and Technology, 23955-6900, Thuwal, Kingdom of Saudi Arabia.*

[c.] *Department of Chemical Engineering, Shanghai Electrochemical Energy Devices Research Center, Shanghai Jiaotong University, 200240, Shanghai, China*

Contents

1. Experimental Section

Synthesis of ZIF

According to the synthesis of ZIF-8, the synthesis of ZIF-Zn is illustrated as follows. First, solution A is prepared. $Zn(NO_3)_2 \cdot 6H_2O$ (5.95 g) was dissolved in 150 mL of methanol as solution A , and 2-methyl imidazole (6.16 g) was dissolved in 150 mL of methanol as solution B. Then, solution B was mixed with solution A and kept stirring at room temperature for 24 hours. The white precipitate was collected by centrifugation, washed by methanol for three times, and then dried in a vacuum oven at 60°C for 12 h, obtaining white powder of ZIF. [1]

Synthesis of MET

According to the synthesis of MET-6, the synthesis of MET is illustrated as follows. First, $ZnCl_2$ (5.0 g) was dissolved in the mixed solvent of 50 mL ethanol, 75 mL water, 20 mL ammonia (25%-28%) and 50 mL N,N-dimethylformamide. Then, 6.26 mL of 1H-1,2,3-triazole was added dropwise in above solution, and kept stirring at room temperature for 24 h. The white precipitate was collected by centrifugation, washed by ethanol for three times, and then dried in a vacuum oven at 80 °C for 8 hours, obtaining the product white powder of MET. [2]

Synthesis of Fe-ZIF and Fe-MET

MET (2.0 g) was immersed into a solution of $FeCl_2 \cdot 4H_2O$ (0.98 g) in 200 mL of methanol. The mixture was ultrasonic treated for 5-10 mins at 80kHz. Then, the mixture was stirred at room temperature for 6 h. The white precipitate was collected by centrifugation, washed by ethanol for three times, and then dried in a vacuum oven at 100 °C for 8 hours.

The synthesis of Fe-ZIF is similar with the process of Fe-MET through the replacing MET by ZIF powders.

Synthesis of Fe@NC and Fe@NCS

The as-synthesized MET, Fe-ZIF and Fe-MET were put into the porcelain boat respectively, and heated from room temperature to 900 °C in tube furnace under N_2 atmosphere at a heating rate of 5 ℃ $mins^{-1}$. After keeping the temperature of 900 °C for 2h, the powder was naturally cooled to room temperature, the products of NCS, Fe@NC and Fe@NCS were obtained.

2. Characterization

The powder X-ray diffraction (XRD) patterns were performed to characterize the synthetic products using Rigaku with Cu Kα, scan range of 5°-70° with a scanning rate of 1 °/min. The BET specific surface area was measured by nitrogen adsorption and desorption at 77 K by ASAP 2020 sorption system. The pore diameter curves of the three samples are determined by QS-DFT methods. Raman spectroscopy of the samples was obtained by a Renishaw in Via Raman Microscope. The X-ray Photoelectron Spectroscopy (XPS) was used to detect the surface composition of the sample on Thermo ESCA Lab250XI. The morphology of the samples was observed by field emission scanning electron microscopy (SEM, verial 460) and transmission electron microscope (TEM, HITACHI HT-7700). High-annular dark-field scanning TEM (HAADF-STEM) and EDX elemental mapping were acquired on FEI Themis G2 transmission electron microscope.

3. Electrochemical Measurement

The active materials (NCS, Fe@NC and Fe@NCS), conductive agent (Ketjen Black) and binder (PVDF) used to prepare the working electrode are mixed in a mass ratio of 8:1:1, and N-methyl-1-2-pyrrolidone (NMP) was used as solvent to make a uniform slurry, which was coated on aluminum foil to make a working electrode with a diameter of 14mm, and then, put it in a vacuum drying oven at 80 °C for 24h. [3] Finally, the half-cell is assembled in an argon filled glove box (water oxygen value less

than 0.01 ppm). The counter electrode uses a sodium sheet with a diameter of 14 mm, glass fiber paper as a diaphragm, and 1 M $NaClO_4$ in Ethylene Carbonate (EC) and diethyl carbonate (DEC) (1:1, v/v) with the addition of 5 wt% fluoroethylene carbonate (FEC) as electrolyte to assemble CR 2032.[5] Galvanostatic charge/discharge measurements of the assembled cells were performed on a CT2001A testing system (Land CT2001A) at room temperature. A CHI600E electrochemical workstation was used to measure the cyclic voltammetry (CV) curves and electrochemical impedance spectroscopy (EIS) spectra. CV curves were acquired at voltages ranging from 0.1 to 3 V. EIS was recorded in the working frequency range of 0.01 Hz to 100 kHz. The Nyquist plots are fitted to a simplified Randles equivalent circuit model to obtain the series resistance (R_s), constant-phase element (CPE) and charge-transfer resistance (R_{ct}).[6] The simplified Randles equivalent circuit model can be expressed as follows:

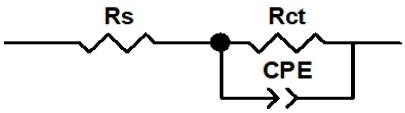

4. Results and Discussions

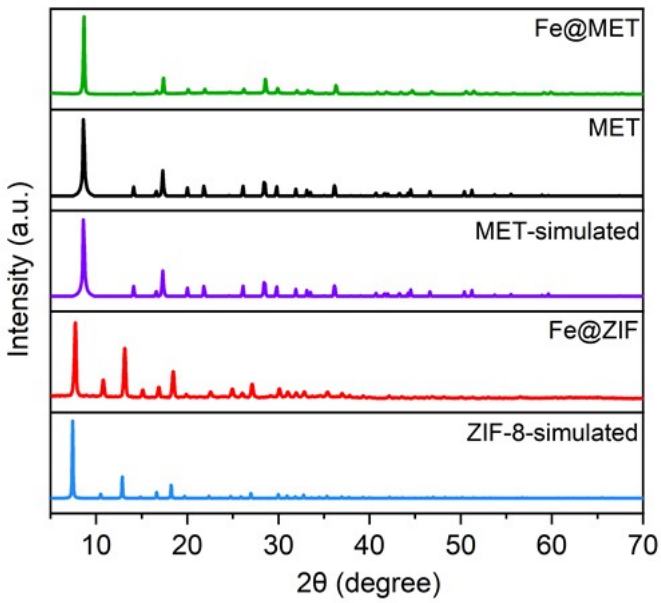

Figure S1. XRD patterns of Fe-MET, MET, MET-simulated, Fe-ZIF and ZIF-8-simulated.

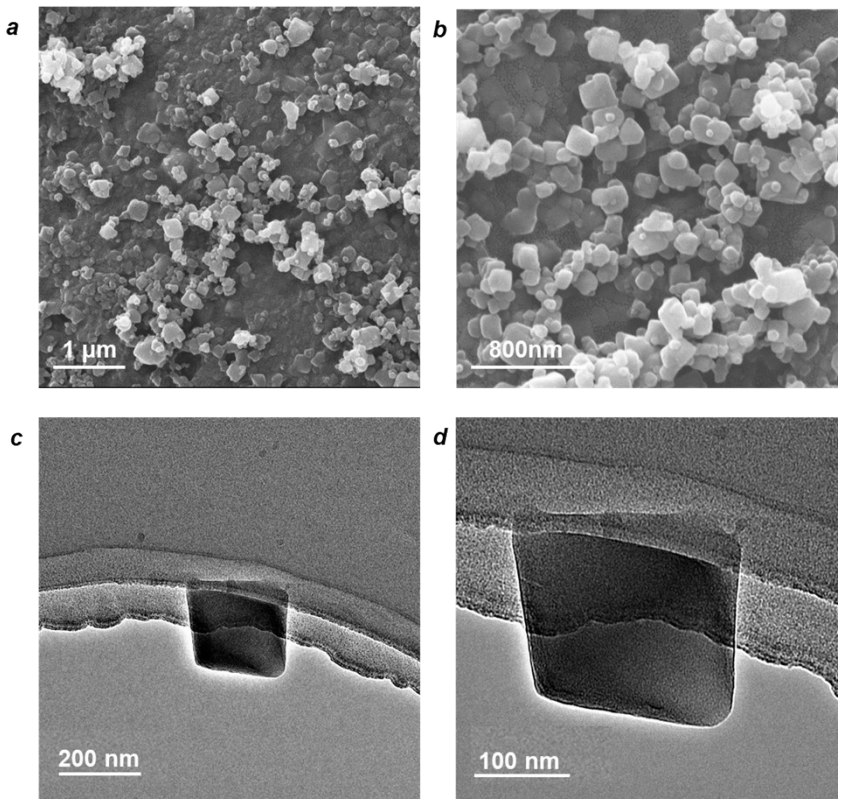

Figure S2. SEM image (a.b,c) and TEM image (d) of Fe-MET

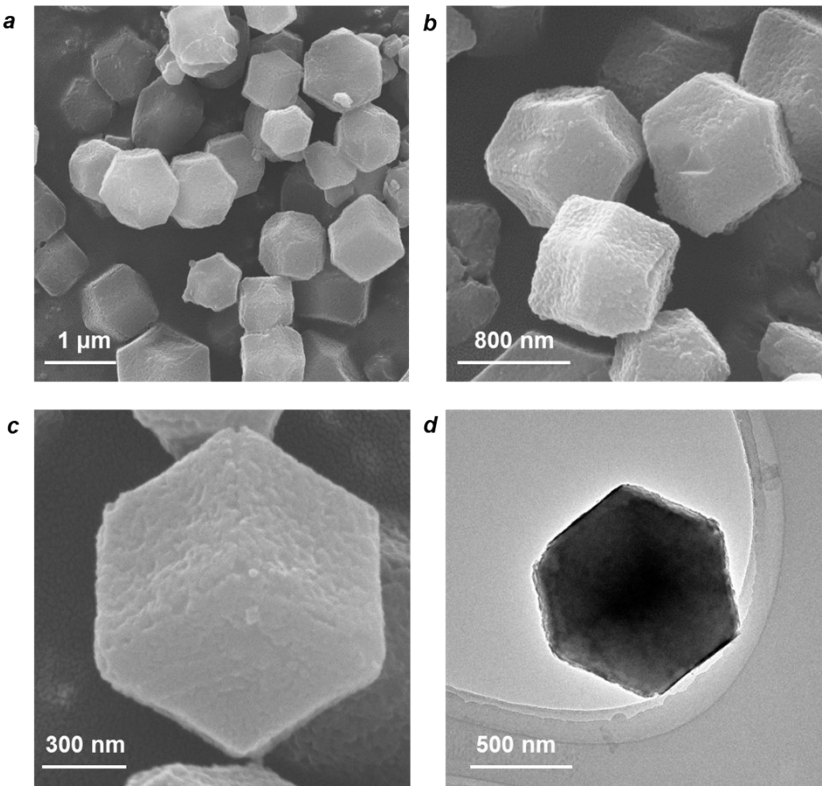

Figure S3. SEM image (a,b,c) and TEM image (d) of Fe@ZIF

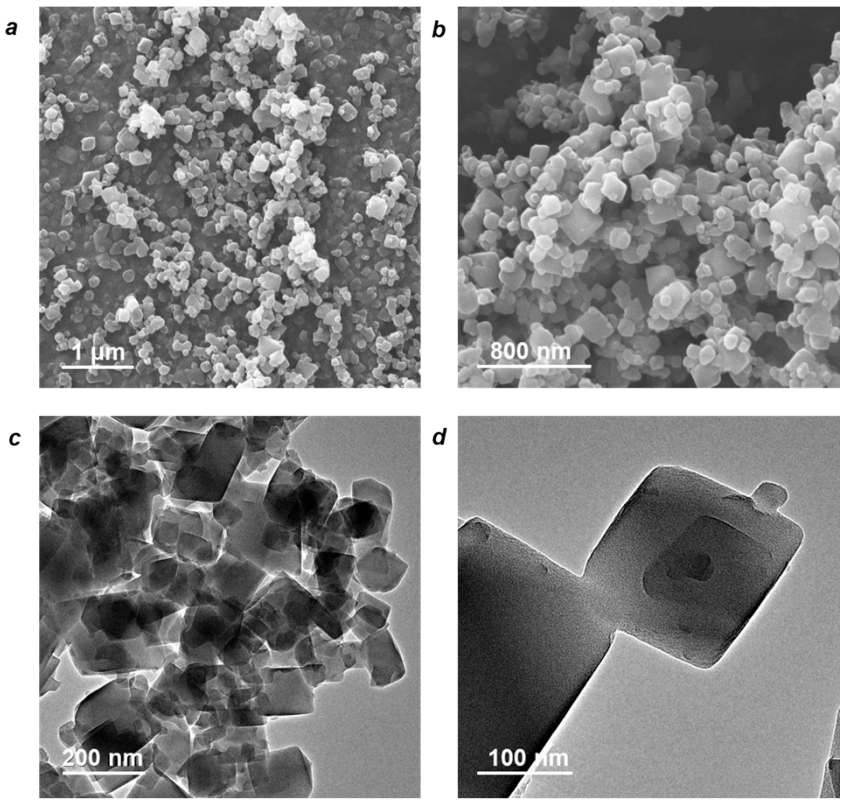

Figure S4. SEM image (a,b) and TEM image (c,d) of MET

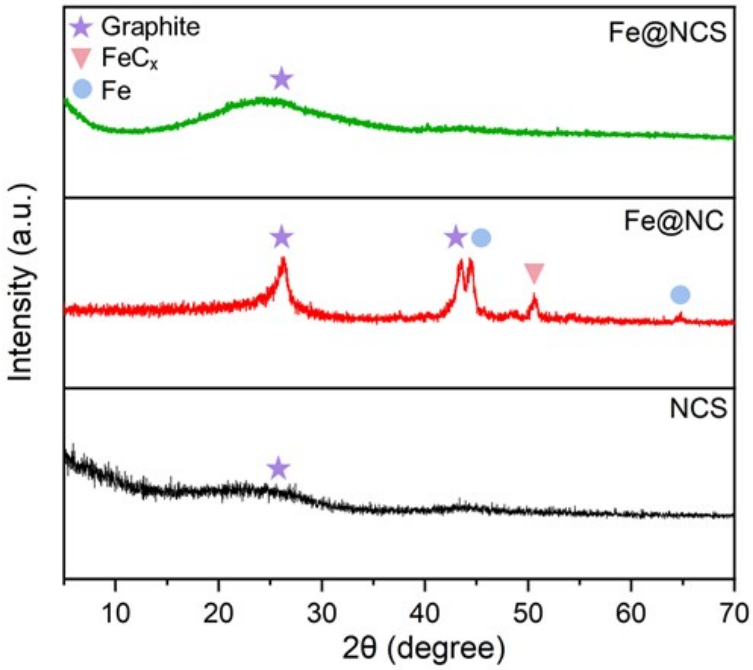

Figure S5. XRD patterns of Fe@NCS, Fe@NC and NCS, JCPDS for graphitic carbon is JCPDS 41-1487, JCPDS for Fe is JCPDS 06-0696, JCPDS for FeC_x (Fe_3C) is JCPDS 35-0772.

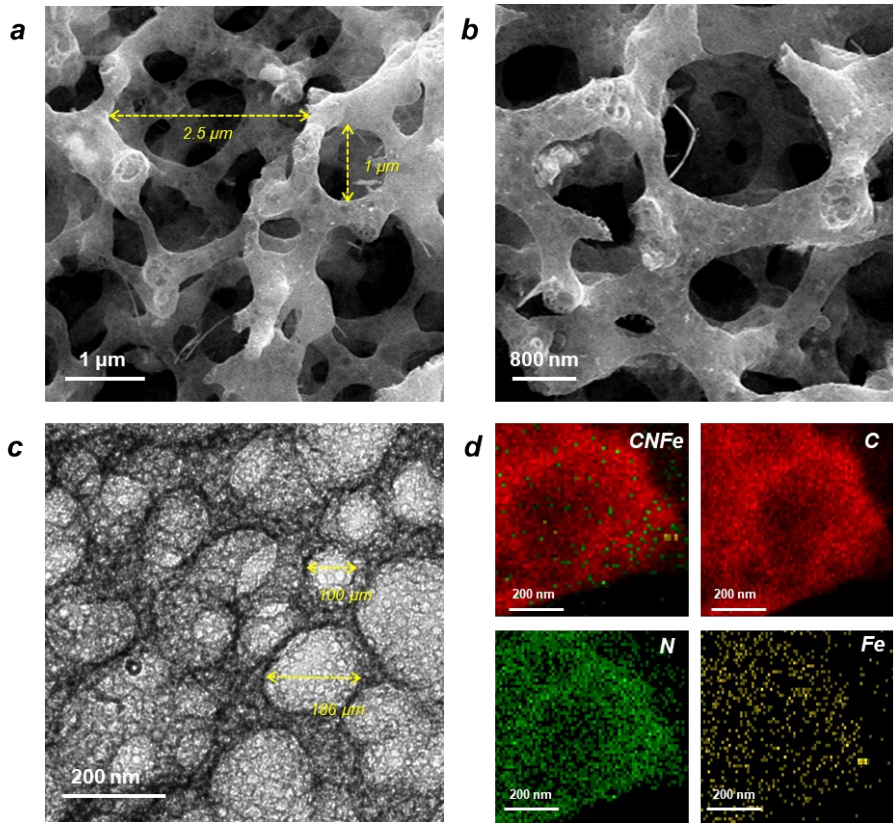

Figure S6. SEM image (a,b) and TEM image (c) of Fe@NCS, EDS mapping of Fe@NCS (d)

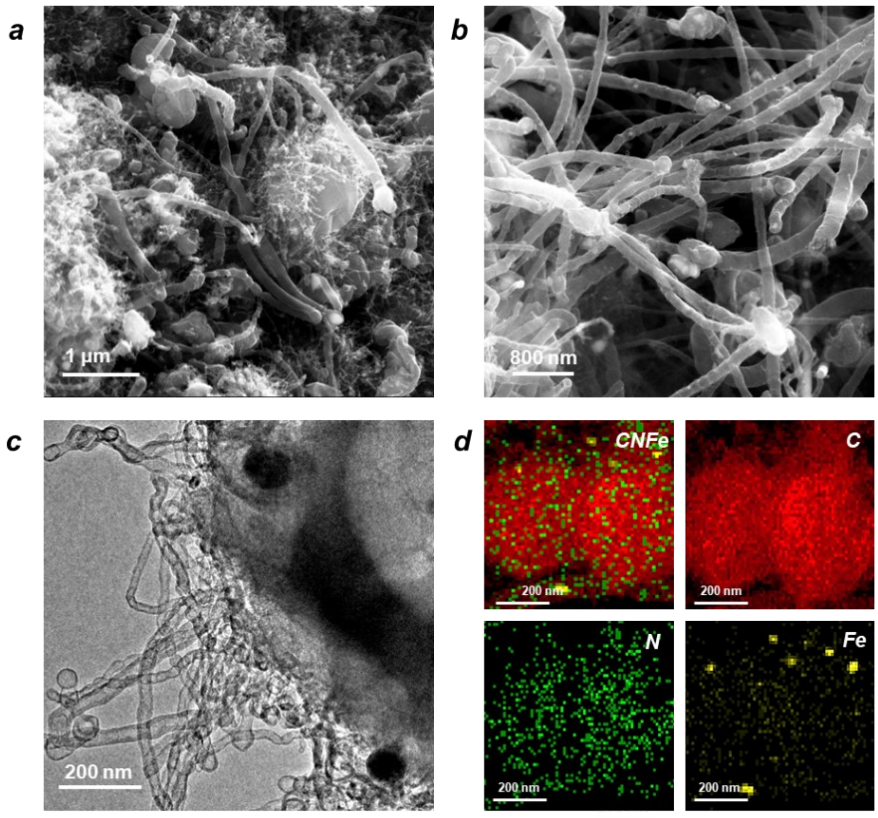

Figure S7. SEM image (a,b) and TEM image (c) of Fe@NC, EDS mapping of Fe@NC (d)

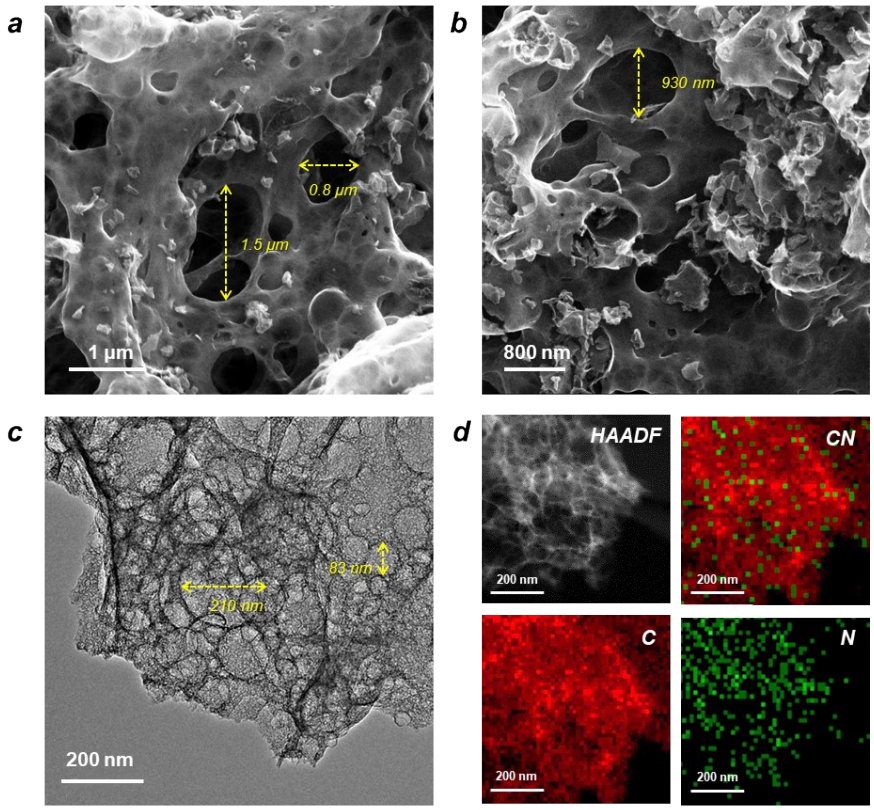

Figure S8. SEM image (a, b) and TEM image (c) of NCS, HAADF and EDS mapping of NCS (d)

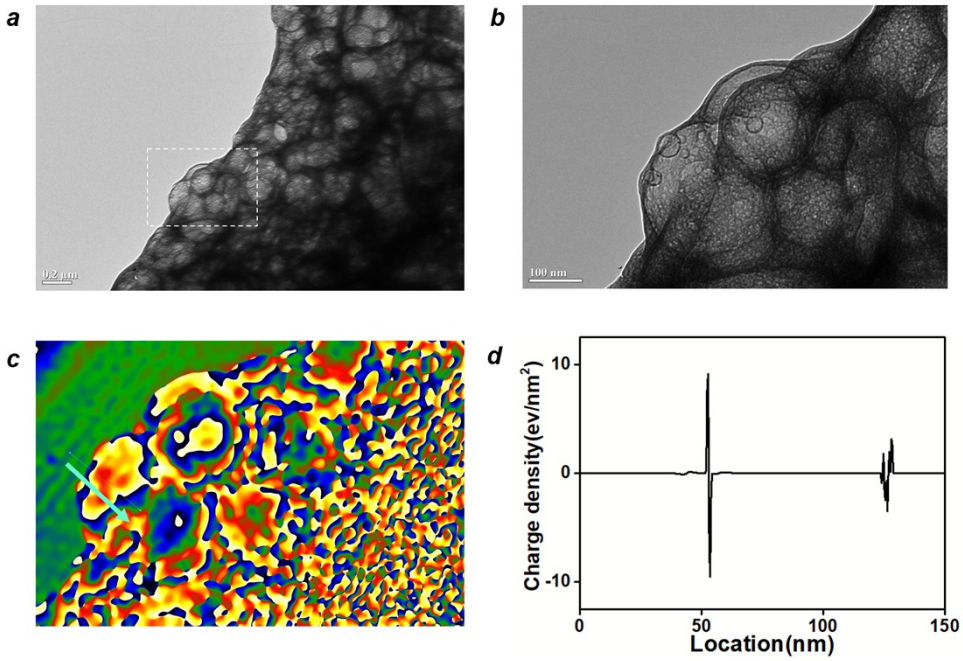

Figure S9. HR-TEM and its corresponding hologram images (a-b), charge density map (c), the profile of charge density in the region along the light green arrow (d) of Fe@NCS.

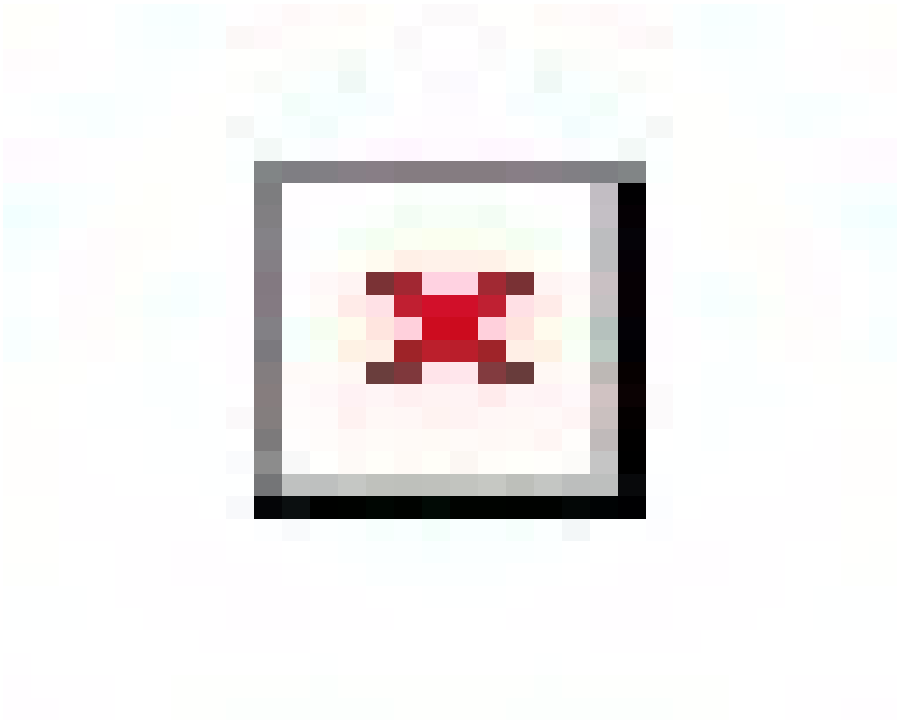

Figure S10. Raman spectra of Fe@NCS, Fe@NC and NCS.

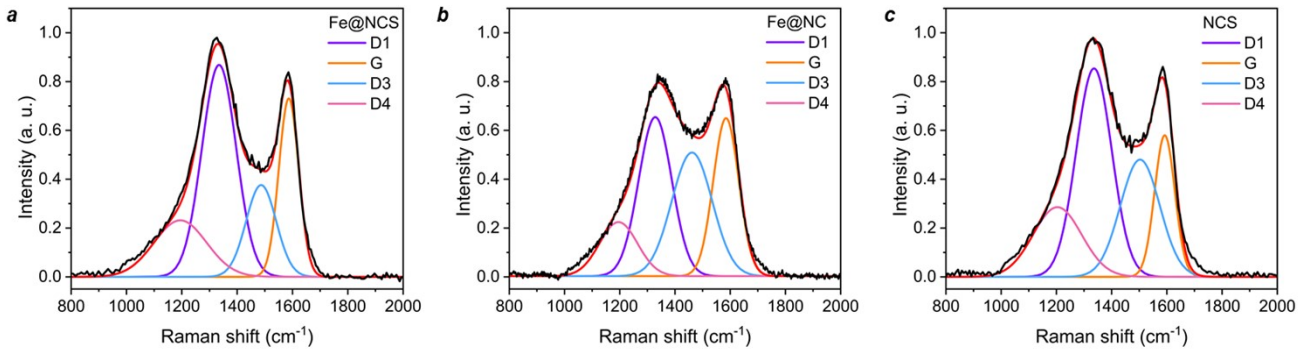

Figure S11. Deconvolution of D and G spectral regions for Fe@NCS, Fe@NC and NCS.

Table S1 Raman shift and area of Raman bands.

Sample	*D1* (cm^{-1})	A_{D1}	*G* (cm^{-1})	A_G	A_{D3}	I_{D1}/I_G	d_{nc} (nm)
Fe@NCS	1335	135.4	1587	65.8	51.4	1.17	1.5
Fe@NC	1329	98.0	1585	75.0	93.2	1.00	1.3
NCS	1336	137.9	1592	53.1	86.1	1.14	1.4

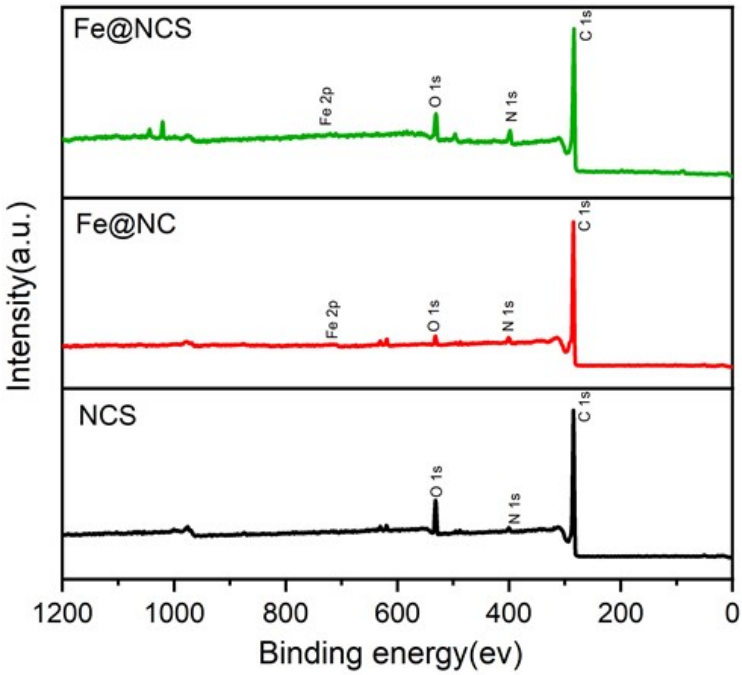

Figure S12. XPS spectra: survey spectrum of Fe@NCS, Fe@NC and NCS.

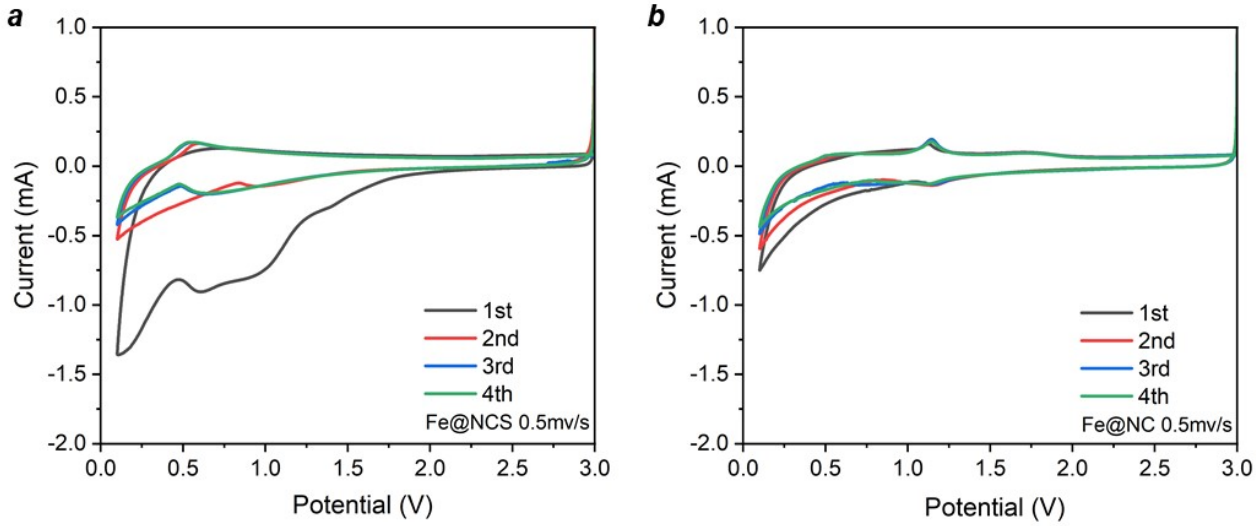

Figure S13. Cyclic voltammetry curves of Fe@NCS (a) and Fe@NC (b) composite electrodes when the scan rate of the first four cycles is 0.5 mv/s.

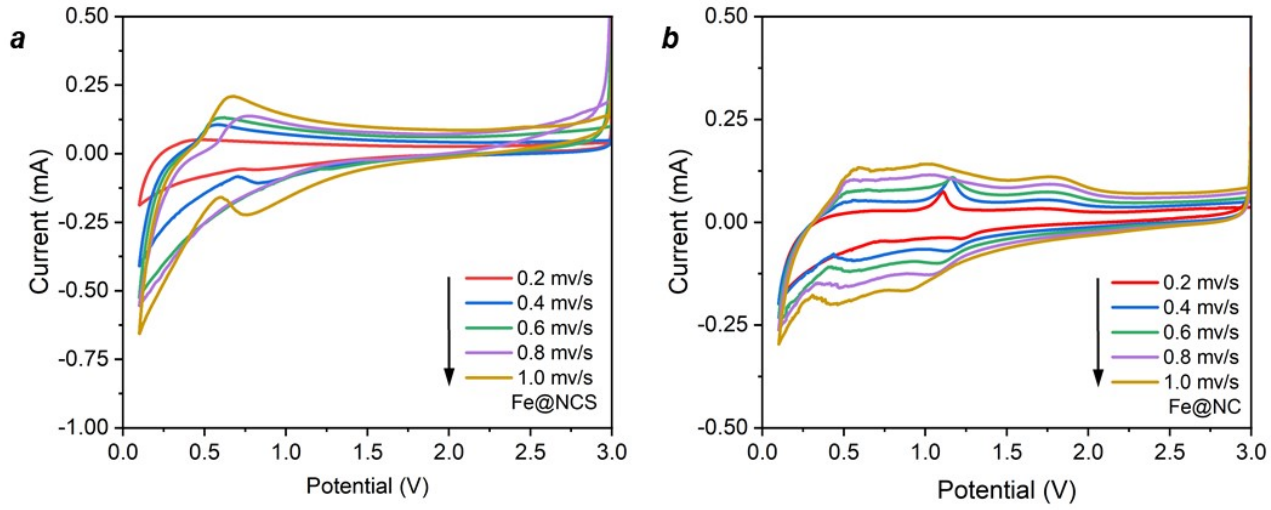

Figure S14. Cyclic voltammetry curves of Fe@NCS (a) and Fe@NC (b) electrodes at different scan rates.

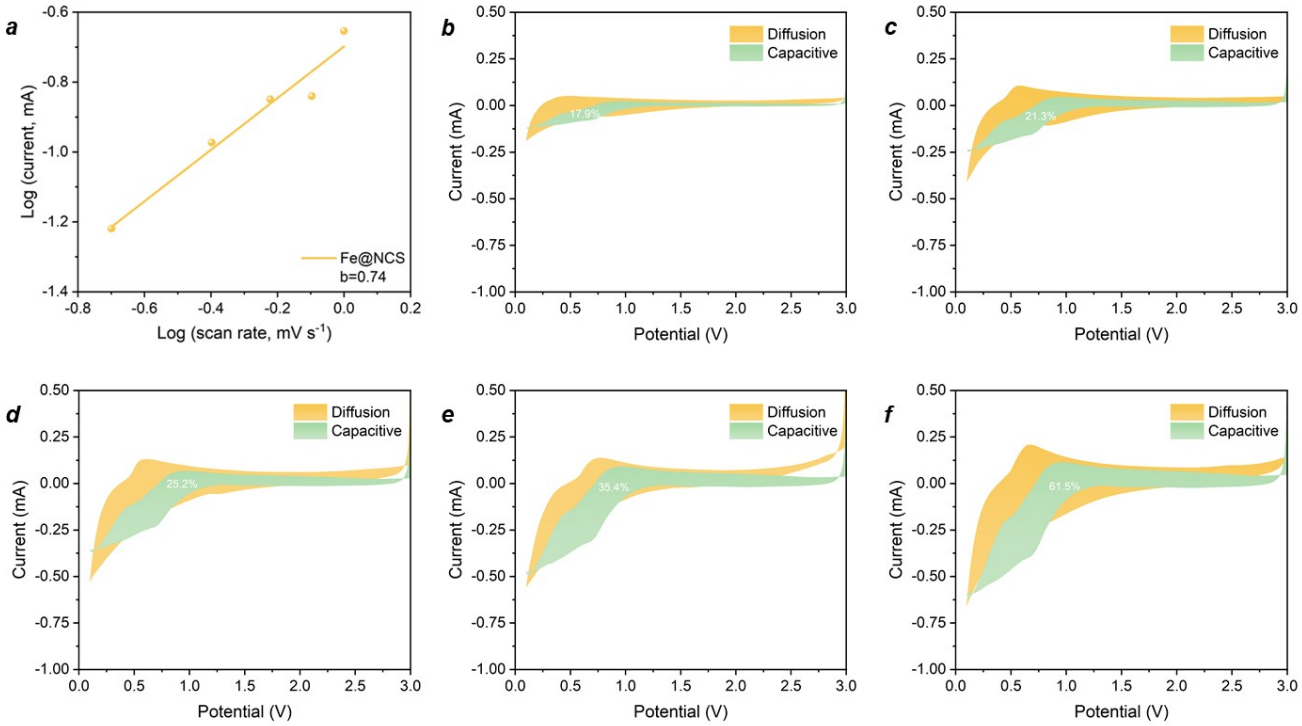

Figure S15. (a) Determine the reaction mechanism of Fe@NCS, calculate the b value, use Log v as the abscissa and Log i as the ordinate; When the scan rate is 0.2(b), 0.4(c), 0.6(d), 0.8(e),1(f) mv/s, Fe@NCS electrode capacity control contribution and diffusion control contribution distribution diagram.

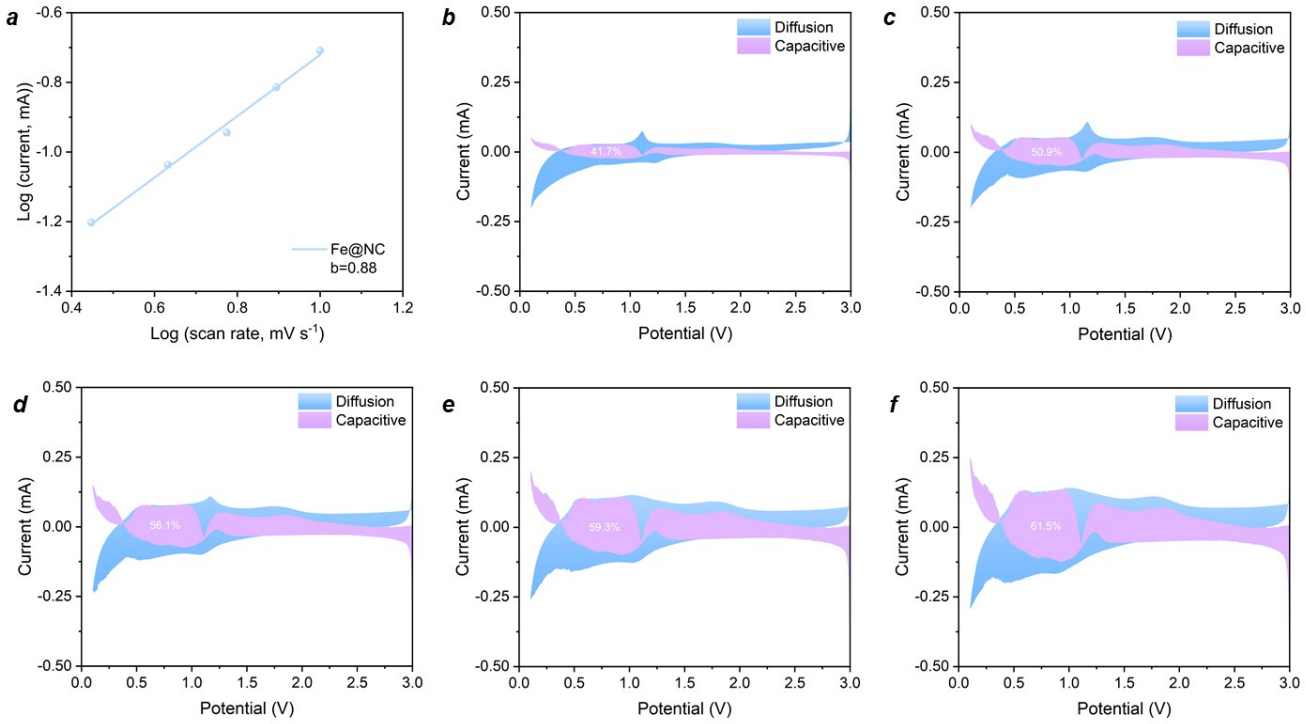

Figure S16. (a) Determine the reaction mechanism of Fe@NC, calculate the b value, use Log v as the abscissa and Log i as the ordinate; When the scan rate is 0.2(b), 0.4(c), 0.6(d), 0.8(e),1(f) mv/s, Fe@NC electrode capacity control contribution and diffusion control contribution distribution diagram.

5. References

[1] H. Wang, H. B. Xu, K. Jia, and R. B. Wu, *ACS Appl. Energy Mater.,* 2019, **2**, 531−538.

[2] R. Zhao, Z. B. Liang, S. Gao, C. Yang, B. J. Zhu, J. L. Zhao, C. Qu, R. Q. Zou and Q. Xu, *Angew. Chem. Int. Ed.,* 2018, 57, 1–6.

[3] X. J. Xu, J. Liu, J. W. Liu, L. Z. Ouyang, R. Z. Hu, H. Wang, L. C. Yang and M. Zhu, *Adv. Funct. Mater.*, 2018, **28**, 1707573.

[4] H. Liu, H. Guo, B. H. Liu, M. F. Liang, Z. L. Lv, K. R. Adair and X. L. Sun, *Adv. Funct. Mater.,* 2018, **28,** 1707480.

[5] L. Q. Wang, Z. L.Han, Q. Q. Zhao, X. Y. Yao, Y. Q. Zhu, X. L. Ma, S. Wu and C. B. Cao, *J. Mater. Chem. A*., 2020, **8**, 8612-8619.

[6] X. Y. Yue, J. J. Wang, Z. K. Xie, Y. He, Z. Liu, C. L. Liu, X. G. Hao, A. Abudula and G. Q. Guan, *ACS Appl. Mater. Interfaces.,* 2021, **13**, 26046−26054.